SCIENCE CHINA
Physics, Mechanics & Astronomy

• Article •

October 2013 Vol.56 No.10: 1952–1961
doi: 10.1007/s11433-013-5257-4

Theoretical analysis of effects of boundary layer bleed on scramjet thrust

YUE LianJie*, XU XianKun & CHANG XinYu

State Key Laboratory of High Temperature Gas Dynamics, Institute of Mechanics, Chinese Academy of Sciences, Beijing 100190, China

Received December 8, 2012; accepted February 18, 2013

The effects of boundary layer bleed on the scramjet thrust are studied in the present paper. A theoretical model is developed to evaluate the thrust increment and influencing factors. The thrust increment resulting from the bleed is dominated by the rise in total pressure recovery and bleed mass flow rate. The bleed mass flow rate exerts stronger impact on the engine thrust than the total pressure. According to current bleed design, it is a severe challenge for the engine to enhance its total pressure to maintain the original thrust when there is no bleeding. Furthermore, the initial total pressure recovery, fuel mass addition, combustion efficiency and area ratio of engine exit to entrance can affect the contributions of the bleeding to the thrust increment. The scramjet needs a higher rise in total pressure recovery to counteract the negative effect of bleed mass loss at higher initial total pressure recovery or larger area ratio of engine exit/entrance. More heat release results in a little lower demand on the rise in total pressure recovery for maintaining the scramjet thrust. These results will aid in understanding the fundamental mechanism of bleeding on engine thrust.

scramjet, boundary layer bleed, theoretical analysis, engine thrust

PACS number(s): 47.85.ld, 47.85.Kn, 47.40.Ki

Citation: Yue L J, Xu X K, Chang X Y. Theoretical analysis of effects of boundary layer bleed on scramjet thrust. Sci China-Phys Mech Astron, 2013, 56: 1952–1961, doi: 10.1007/s11433-013-5257-4

1 Introduction

Scramjet engines are expected to be a promising candidate of the propulsion unit for future space transportation systems. The internal flow path features some complex flow phenomena. Different types of irreversible processes are involved, such as shocks and shock-induced boundary layer separations [1]. The boundary layer might be separated by strong shock waves, which are always associated with some types of losses, including drag increase and pressure recovery losses. The separations near the inlet throat can possibly trigger the inlet unstart and promote engine stall. In particular, the flow control of shock-induced separations within a hypersonic inlet has been identified to be critical for achieving the desired flow performances.

To avoid boundary-layer separation and prevent engine unstart, boundary layer bleed was widely adopted as the most common technique in existing supersonic aircrafts or ramjet-powered missiles [2]. Much research has been carried out on the effect of boundary layer bleed on inlet performance [3–10]. Bleeding away the near-wall boundary layer at certain locations not only improves pressure recovery, but also reduces shock instabilities and extends the maneuvering range. The bleed configuration has been optimized and the influence of geometry on the bleed efficiency has been examined, such as porous sections, slots or scoops and various angle of bleed holes [3,7,8]. The fundamental studies regarding shock-wave boundary-layer interaction with different bleed systems were also carried out by Hamed et al. and Shih et al. to facilitate its design [11–14].

*Corresponding author (email: yuelj@imech.ac.cn)

As one of the most powerful methods to suppress boundary layer separations, the bleed systems were subsequently introduced into scramjet design [15–27]. Mitani showed that bleeding of 0.65% in captured airflow suppressed effectively the boundary layer separation, improved the unstart characteristics in engines and doubled the engine operating range [15–17]. Häberle and Gülhan deployed a passive boundary layer bleed at the throat of a fixed geometry hypersonic inlet to diminish significantly the lip shock-induced separation bubble on the ramp and reduce the risk of inlet unstart with 5% mass flow rate penalty [18–20]. Falempin [21] and Pandian [22] also adopted perforation bleed as an efficient method to ensure air-inlet starting and improve their overall characteristics. Schulte examined the application of boundary layer bleed for the improvement of hypersonic inlet efficiency [23,24]. The implementation of bleed leads to a reduction of the separation bubble thickness by almost 50%, as well as a reduction in related vortex-induced highly localized thermal loads. Additionally, Weiss investigated the interaction of a shock train with a normal suction slot in a scramjet isolator [25]. It was concluded that the back pressure of the shock train can be increased until the shock train gradually changes into a single normal shock because of the suction stabilized primary shock foot. The suction mass flow is a significant parameter in shock stabilization.

Proper design of the bleed system is of great importance for the performance of scramjet engine. Note that the boundary layer bleed can increase the total pressure recovery and stabilize the flow, which tends to improve scramjet engine performance. Conversely, the gain in total pressure recovery is achieved at the expense of a captured mass flow loss, which tends to reduce scramjet thrust under stable engine operations. Previous research indicates that the scramjet engine thrust margin is severely limited. Any technique should be employed prudently if one attempts to maintain the engine thrust as high as possible. Hence, research has been devoted to the bleed configuration optimization, which generally maximizes the total pressure or minimizes the mass flow loss. Schulte proposed certain favorable schemes for the bleed configuration [24]. A position of the bleed slot directly upstream of the shock impingement location was identified to be the most effective. Tam studied the effects and performance of different bleed configurations in a scramjet isolator [26]. Nevertheless, the question has not been addressed as of yet to answer how the bleed affects the scramjet engine thrust via changes in total pressure and mass flow loss. Researchers are still considering which aspect they should focus in bleed system designs regarding engine thrust. Therefore, a clear understanding of the impact of boundary layer bleed on scramjet thrust is of critical importance to refine this control technique.

The main objective of this study is to clarify the comprehensive influence of the boundary layer bleed on the scramjet engine thrust. This paper makes a detailed theoretical analysis of the impact of bleeding, specifically the contributions of total pressure rise and mass flow loss to the variation of engine thrust, as well as the influence of some other parameters. An assessment of the boundary layer bleed impact was then conducted, and the effects of various factors are also surveyed.

2 Analytical model for engine thrust

This section details the general expression of the scramjet thrust. Figure 1 shows the sketch of the scramjet flow path with a boundary layer bleed. Station 1-1' represents the engine entrance, station 3-3' denotes the engine exit. Generally, the engine exit flow is non-uniform. Three-dimensional flows at the exit need be one dimensionalized by stream thrust averaging for parametric performance evaluations without thrust loss. The stream thrust averaging is effectively equivalent to a process in which the distorted 3-D flow passes through an idealized inviscid duct where the flow is completely mixed at station 4-4'. By applying the conservation laws of mass, momentum, energy, the averaged exit flow parameters can be derived.

The following assumptions are made for simplifying the analysis with acceptable accuracy:

(1) The axial stream thrust of the bleed flow is much lower than that of the freestream. This is reasonable because the bleed air of the scramjet has always been exhausted directly to the atmosphere at a low plenum pressure [15–24].

(2) Combustion efficiency is irrelevant to the boundary layer bleed. In reality, compared with the inlet captured flow, the bleed mass loss is generally less than 5%, and is too low to change the flow pattern in the burner [15,18]. Accordingly, it is reasonable to ignore the influence of the bleed on the combustion efficiency.

(3) The external compression system is not altered by the boundary layer bleed. Thus the mass capture and spillage drag are not altered. Almost all the bleed system can meet this requirement.

(4) The gas is locally treated as calorically perfect gas. The specific heat ratio varies as the gas components change along the *X*-direction.

The general expression for the engine thrust F can be

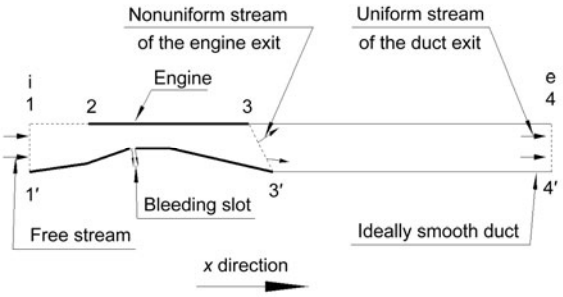

Figure 1 Sketch of the scramjet flow path with a boundary layer bleed.

written as follows:

$$F = (p_e + \rho_e V_e^2)A_e - (p_i + \rho_i V_i^2)A_i + I_{bleed} - D_{spillage}, \quad (1)$$

where p_i, ρ_i, V_i and p_e, ρ_e, V_e represent static pressure, density, velocity at engine entrance and exit with uniform steam, respectively; A_e is cross section area at the engine exit; A_i is area of the captured stream tube in the freestream; I_{bleed} denotes the stream thrust of the bleed flow along freestream direction; $D_{spillage}$ represents the inlet spillage drag.

Based on assumption (1), I_{bleed} can be neglected. By normalizing F with the product of freestream total pressure P_{ti} and A_i, eq. (1) can be rewritten as:

$$F_{nd} = \sigma \frac{A_e}{A_i}\left(1+\frac{\gamma_e-1}{2}M_e^2\right)^{-\left(\frac{\gamma_e}{\gamma_e-1}\right)}(1+\gamma_e M_e^2) - \left(1+\frac{\gamma_i-1}{2}M_i^2\right)^{-\left(\frac{\gamma_i}{\gamma_i-1}\right)}(1+\gamma_i M_i^2) - \frac{D_{spillage}}{P_{ti}A_i}, \quad (2)$$

where F_{nd} denotes dimensionless thrust $F/P_{ti}A_i$; M_i, γ_i and M_e, γ_e stand for Mach number, specific heat ratio at engine entrance and exit, respectively; σ is total pressure recovery across the engine. The dimensionless inlet spillage drag $D_{spillage}/P_{ti}A_i$ depends on the scramjet geometry and incoming Mach number no matter whether there is a bleed or not.

For a given scramjet, the equation implies the dependence of F_{nd} as:

$$F_{nd} = funct\left(M_i, M_e, \gamma_e, \sigma, A_e/A_i, D_{spillage}/P_{ti}A_i\right). \quad (3)$$

Furthermore, the interrelation among the flow properties at the engine exit is established by mass conservation;

$$\sigma = (1-\varphi+f)\left(1+\frac{\gamma_i-1}{2}M_i^2\right)^{-\frac{(\gamma_i+1)}{2(\gamma_i-1)}}\left(1+\frac{\gamma_e-1}{2}M_e^2\right)^{\frac{(\gamma_e+1)}{2(\gamma_e-1)}} \times \frac{M_i}{M_e}\frac{A_i}{A_e}\sqrt{\frac{\gamma_i}{\gamma_e}\frac{R_e}{R_i}\frac{T_{te}}{T_{ti}}}, \quad (4)$$

where T_{ti} and T_{te} stand for stagnation temperature at engine entrance and exit, respectively; φ represents ratio of the bleed mass flow rate to the inlet captured mass flow rate. The fuel-air mass flow rate ratio f is defined in this article as the ratio of the fuel mass flow rate to the inlet captured mass flow rate. The equation with φ=0 represents the case without bleeding. Eq. (4) indicates that the functional relationship between exit Mach number M_e and other parameters.

From energy conservation:

$$(1-\varphi)C_{pi}T_{ti} + f\eta h_{PR} = (1-\varphi+f)C_{pe}T_{te}, \quad (5)$$

where the enthalpy and the kinetic energy of fuel are negligible compared to the combustion heat release. η stands for combustion efficiency; C_{pe} and C_{pi} denote isobaric specific heat capacity at engine entrance and exit, respectively. Generally, the airbreathing hypersonic vehicles run at the flight altitude from 20 km to 35 km [27]. The atmosphere temperature approximately is kept somewhat constant, and the freestream stagnation temperature T_{ti} is determined by M_i only. Moreover, the specific heat ratio γ_e and isobaric specific heat capacity C_{pe} are determined by gas components and gas temperature, which are related to chemical energy release and scramjet operating condition. As a result, stagnation temperature ratio T_{te}/T_{ti} varies with f, η, φ, M_i.

Through the combination of above equations, the functional dependence of dimensionless thrust F_{nd} for a given scramjet geometry is derived as:

$$F_{nd} = funct\left(M_i, \varphi, f, \sigma, \eta, A_e/A_i, D_{spillage}/P_{ti}A_i\right). \quad (6)$$

This paper evaluates the effect of boundary layer bleed for a fixed fuel supply, that is, f will not vary no matter whether there is a bleed or not. Based on assumption (2), the equivalent heat release is thus transferred to the main gas regardless of the bleed. In the following analysis, the subscript "a" is used to represent the exit flow states without the boundary layer bleed, and subscript "b" denotes those with the bleed.

According to eq. (2), the increment of dimensionless engine thrust due to the bleed can be derived as:

$$\Delta F_{nd} = \sigma_a \frac{A_e}{A_i}\left[\Omega\left(1+\frac{\gamma_{e,b}-1}{2}M_{e,b}^2\right)^{-\left(\frac{\gamma_{e,b}}{\gamma_{e,b}-1}\right)}(1+\gamma_{e,b}M_{e,b}^2) - \left(1+\frac{\gamma_{e,a}-1}{2}M_{e,a}^2\right)^{-\left(\frac{\gamma_{e,a}}{\gamma_{e,a}-1}\right)}(1+\gamma_{e,a}M_{e,a}^2)\right], \quad (7)$$

where Ω is the ratio of total pressure recovery with the bleed to that without the bleed, σ_b/σ_a. It reflects the efficiency of the bleed design, and it is generally greater than 1.0 because the bleed air is considered to be low energy.

As with the derivation above, this offers a functional dependence of dimensionless thrust increment for a given scramjet:

$$\Delta F_{nd} = funct(M_i, \sigma_a, \Omega, \varphi, f, \eta, A_e/A_i). \quad (8)$$

Eq. (8) reveals that, for a scramjet flying at a given freestream Mach number, the thrust increment with the bleed is dominated by the rise in total pressure recovery and the bleed mass flow rate. While some other scramjet operating parameters, including initial total pressure recovery, fuel mass addition, combustion efficiency and area ratio of engine exit/entrance, affect the contribution of the rise in total pressure recovery and the bleed mass flow rate to the thrust.

3 Effects of boundary layer bleed on engine thrust

A calculation is conducted for hydrogen-fueled scramjet to

demonstrate the impact of boundary layer bleed on engine thrust. The scramjet operates at Mach 6.0 and altitude of 25 km. The contributions of the bleed flow loss φ and the total pressure ratio Ω are studied, as well as the influences of various other factors, $\sigma_a, f, \eta, \varphi$.

For simplicity, the gas components are described by the following chemical reaction:

$$2H_2+(O_2+3.76N_2)\rightarrow 2H_2O+3.76N_2. \quad (9)$$

The combustion gas at the engine exit is a mixture of unburned H_2, excess O_2, N_2 and H_2O. The proportion of consumed H_2 to hydrogen supply is equivalent to combustion efficiency η. For unit mass of air flow, consumed hydrogen mass flow rate is $f\eta$ and the unburned H_2 is $f(1-\eta)$. Correspondingly, the mass flow rate of excess O_2, N_2 and H_2O are $0.233-8f\eta$, 0.767, $9f\eta$, respectively. The gas thermodynamic parameters is then determined based on the gas temperature and mass fraction of each component.

3.1 Effect of the bleed at different initial total pressure recovery

The inlet mass capture is assumed to be 100%, and area ratio A_e/A_i through the scramjet is given as 1.5. The equivalence ratio Φ_a is 0.9 and the combustion efficiency is defined as 87% as described elsewhere [28].

Figure 2 shows the dependence of thrust increment $\Delta F/F_a$ on total pressure ratio Ω and bleed mass ratio φ at different initial total pressure recovery σ_a. $\Delta F/F_a$ denotes $\Delta F_{nd}/F_{nd,a}$, which represents the percentage of the thrust increment. It can be observed that the engine thrust increases with the total pressure ratio Ω at a constant bleed mass ratio φ. Undoubtedly, the engine thrust can be boosted if the bleed is well designed so that higher total pressure is achieved. In other words, the engine thrust will fall if more bleed mass is consumed for a constant total pressure rise. A black line is also illustrated in each figure, which represents the state ΔF=0. This indicates the state in which the engine thrust does not vary with the boundary layer bleed because the gain in the engine thrust because of total pressure rise just balances the thrust drop because of the mass flow loss. The black line divides the figure into two zones. Above the line $\Delta F/F_a$ is negative, indicating that the boundary layer bleed degrades the thrust, whereas beneath the line $\Delta F/F_a$ is positive, illustrating that the boundary layer bleed augments the thrust. Note that, the mass flow rate exerts stronger impact on the engine thrust than the total pressure does in the present case. As an example, at σ_a =0.05, the total pressure ratio Ω needs to reach 1.06 or more to allow the engine thrust unchanged for a bleed with merely 1% mass flow loss. This offers strict demand on total pressure improvement to maintain the thrust. Furthermore, the total pressure ratio Ω increases approximately linearly with the bleed mass loss φ along the black line $\Delta F/F_a$=0. The total pressure recovery need be raised more to make up the larger bleed mass loss so as not to reduce engine thrust.

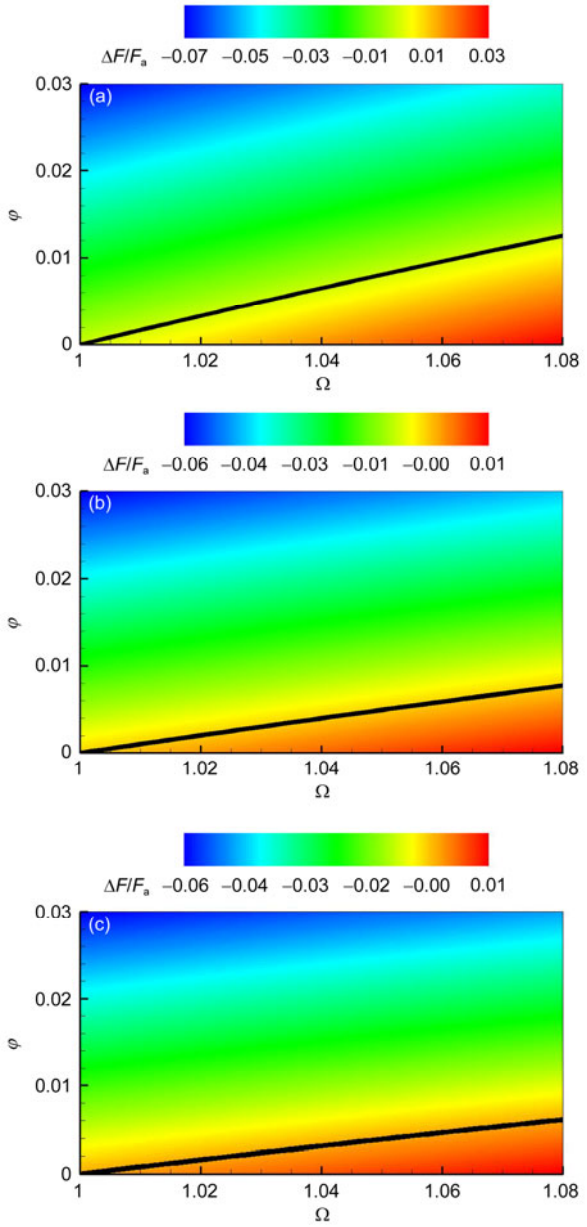

Figure 2 Variation of $\Delta F/F_a$ with φ and Ω at different σ_a. (a) σ_a=0.05; (b) σ_a = 0.1; (c) σ_a =0.15.

Figure 3 plots the lines ΔF=0 at four different initial total pressure recovery σ_a. It is evident that lower σ_a leads to an expansion of the area in which there is positive thrust increment. At σ_a=0.05, the engine thrust can rise when the total pressure recovery increase 1.037 times to 5.18% for 0.6% bleed mass flow loss. At σ_a=0.1, the total pressure ratio reaches 1.06 on the line $\Delta F/F_a$=0. That is, the engine thrust will fall with the boundary layer bleed un1ess the increase of total pressure recovery exceeds 6% of the initial total pressure recovery. This implies that the boundary layer bleed should be designed with increased sophistication

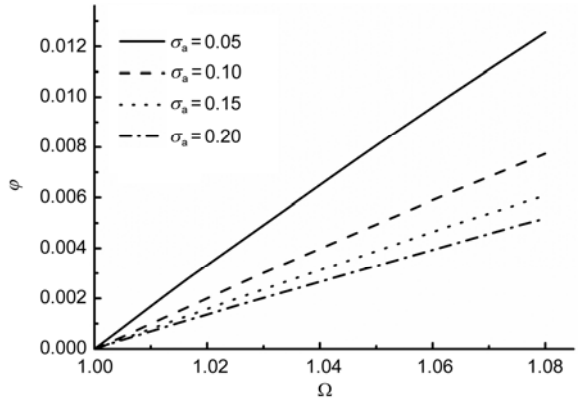

Figure 3 Comparison of lines ΔF=0 at different σ_a.

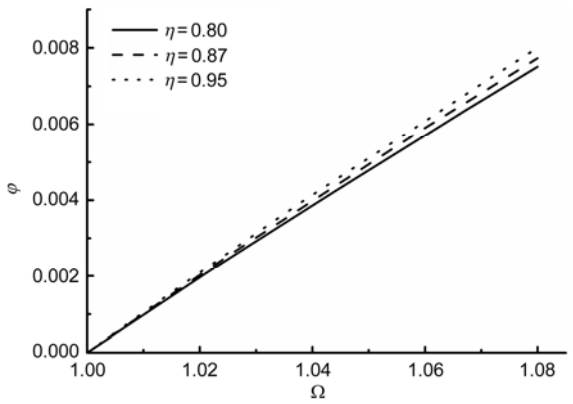

Figure 5 Comparison of lines ΔF=0 at different η.

when the scramjet operates at a higher total pressure recovery, otherwise the engine thrust would be decreased.

3.2 Effect of the bleed at different combustion efficiency

According to Yu et al. [28], the up-to-date combustion efficiency in a scramjet is larger than 80%. Here we specified it as 80%, 87% and 95% to discuss the effect at $\sigma_a = 0.1$.

Figures 2(b) and 4 show the dependence of thrust increment $\Delta F/F_a$ on total pressure ratio Ω and bleed mass ratio φ for different combustion efficiency η. The figures exhibit variations of thrust increment similar to those in Figure 2. Figure 5 further plots the lines ΔF=0 at three different combustion efficiency η, which manifests that the bleed is able to reap more benefit in thrust increase at higher combustion efficiency. At the same bleed mass loss, less total pressure rise is sufficient for a scramjet to maintain the engine thrust at higher combustion efficiency. This implies that the bleed design confronts more severe challenges for benefiting engine thrust when the practical scramjet runs at lower combustion efficiency. Of course, the influence of the combustion efficiency is not great in the present case.

3.3 Effect of the bleed with addition of fuel mass

The combustion efficiency is specified as 87% and the initial total pressure recovery σ_a is 0.1.

Figure 6, in combination with Figure 2(b), shows the dependence of thrust increment $\Delta F/F_a$ on total pressure ratio Ω and bleed mass ratio φ for the fuel equivalence ratio Φ_a of 0.7, 0.9, respectively. As in the preceding sections, the figures exhibit similar variations of thrust increment. Figure 7 further plots the lines ΔF=0 for three different fuel equivalence ratio Φ_a. It indicates that the bleed is apt to achieve thrust growth with more addition of fuel mass.

At the same bleed mass, little less total pressure rise is sufficient for a scramjet to hold the engine thrust at a larger fuel equivalence ratio. The tendency is similar to that for combustion efficiency. Either fuel equivalence ratio or combustion efficiency is associated with the heat release, and has the same role as heat addition except that different fuel supplies alter slightly the combustion gas mass flow rate. It is difficult for the bleed design to maintain the engine thrust at a small combustion heat release.

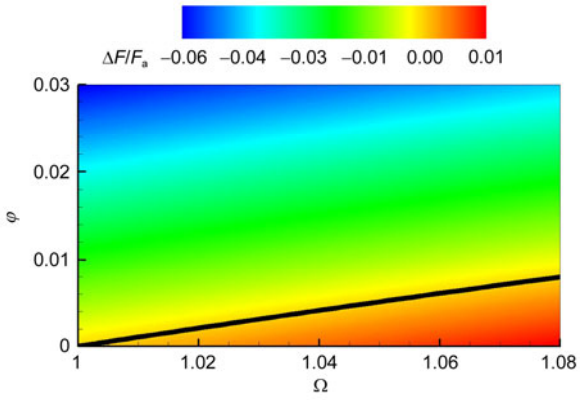

Figure 4 Variation of $\Delta F/F_a$ with φ and Ω at different η. Combustion efficiency $\eta = 0.95$.

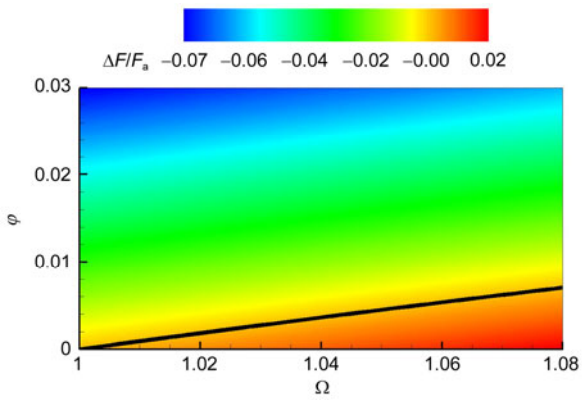

Figure 6 Variation of $\Delta F/F_a$ with φ and Ω at different Φ_a. Equivalence ratio $\Phi_a = 0.7$.

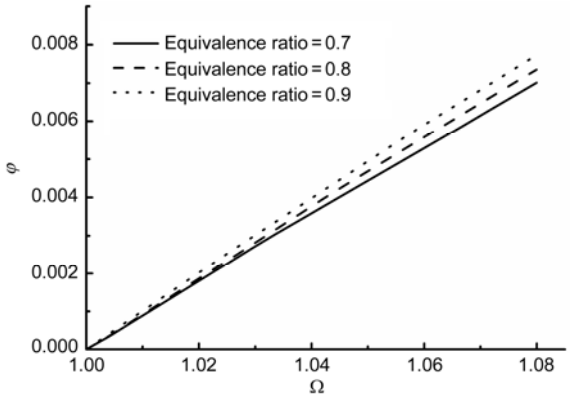

Figure 7 Comparison of lines ΔF=0 at different Φ_a.

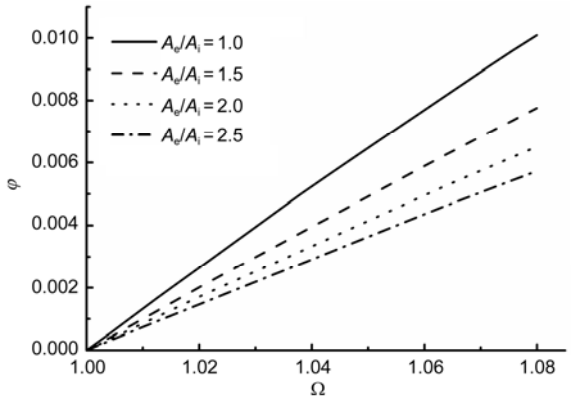

Figure 9 Comparison of lines ΔF=0 at different A_e/A_i.

3.4 Effect of the bleed at different area ratio A_e/A_i

The combustion efficiency is specified as 87% and the fuel equivalence ratio as 0.9. The initial total pressure recovery σ_a is set as 0.1.

Figure 8, together with Figure 2(b), shows the dependence of thrust increment $\Delta F/F_a$ on total pressure ratio Ω and bleed mass ratio φ for different area ratios A_e/A_i, respectively. Figure 9 further plots the lines ΔF=0 at four different area ratios. Note that it is more difficult for the scramjet to benefit from the bleed at larger area ratio A_e/A_i. At the same bleed mass, the engine with larger area ratio A_e/A_i needs much more total pressure rise to maintain the engine thrust. Generally, the flow would accelerate sufficiently to obtain sufficient thrust at a large area ratio A_e/A_i. Hence, the flow mass rate has a more critical role in engine thrust.

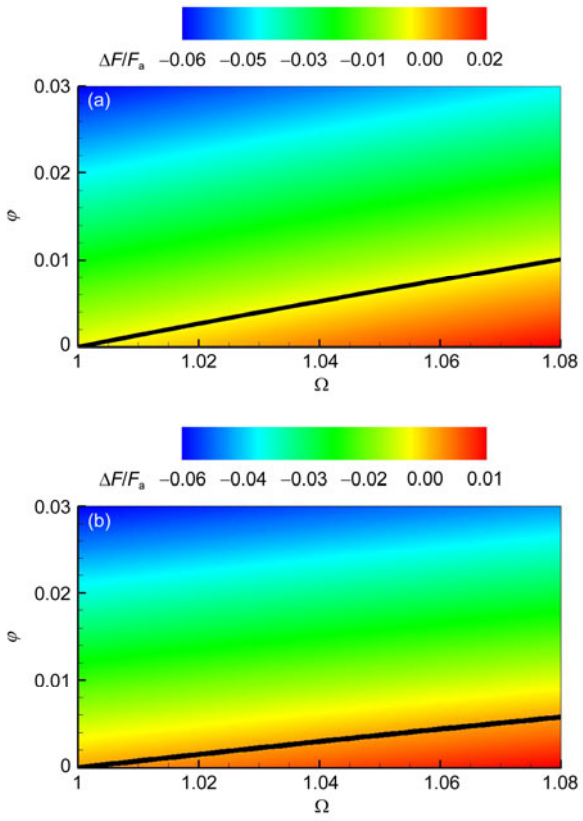

Figure 8 Variation of $\Delta F/F_a$ with φ and Ω at different A_e/A_i. (a) A_e/A_i=1.0; (b) A_e/A_i=2.5.

4 Mathematical analysis of the effects of key factors

Some phenomena have been observed in Section 3 regarding the influence of bleed on engine thrust. There is still some doubt regarding the universality of the aforementioned tendency.

Figure 10 shows the line $\Delta F/F_a$=0, on which a bleed mass ratio φ_z corresponds to a total pressure ratio Ω_z. This section analyzes the variation of Ω_z versus different factors at a fixed bleed mass ratio φ_z to check the tendency given in Section 3.

From eq. (6), the equation describing line ΔF_{nd}=0 can be written as:

$$\Omega_z\left(1+\frac{\gamma_{e,b}-1}{2}M_{e,b}^{\ 2}\right)^{-\left(\frac{\gamma_{e,b}}{\gamma_{e,b}-1}\right)}(1+\gamma_{e,b}M_{e,b}^{\ 2})$$
$$=\left(1+\frac{\gamma_{e,a}-1}{2}M_{e,a}^{\ 2}\right)^{-\left(\frac{\gamma_{e,a}}{\gamma_{e,a}-1}\right)}(1+\gamma_{e,a}M_{e,a}^{\ 2}). \quad (10)$$

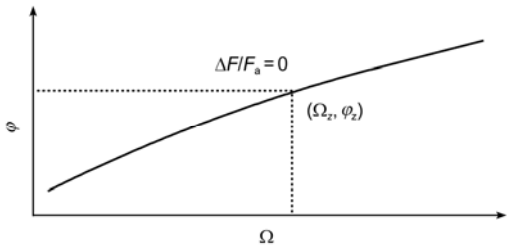

Figure 10 Line $\Delta F/F_a$=0 on coordinate plane (Ω,φ).

With reference to eq. (4), the following two expressions describe mass conservation for the case with and without the bleed, respectively

$$\Omega_z = \frac{1}{\sigma_a}(\varphi_z + f)M_i\left(1+\frac{\gamma_i-1}{2}M_i^{\,2}\right)^{-\frac{(\gamma_i+1)}{2(\gamma_i-1)}} \frac{1}{M_{e,b}}\left(1+\frac{\gamma_{e,b}-1}{2}M_{e,b}^{\,2}\right)^{\frac{(\gamma_{e,b}+1)}{2(\gamma_{e,b}-1)}} \frac{A_i}{A_e}\sqrt{\frac{\gamma_i}{\gamma_{e,b}}\frac{R_{e,b}}{R_i}\frac{T_{te,b}}{T_{ti}}}, \quad (11)$$

$$\sigma_a = (1+f)M_i\left(1+\frac{\gamma_i-1}{2}M_i^{\,2}\right)^{-\frac{(\gamma_i+1)}{2(\gamma_i-1)}} \times\frac{1}{M_{e,a}}\left(1+\frac{\gamma_{e,a}-1}{2}M_{e,a}^{\,2}\right)^{\frac{(\gamma_{e,a}+1)}{2(\gamma_{e,a}-1)}} \frac{A_i}{A_e}\sqrt{\frac{\gamma_i}{\gamma_{e,a}}\frac{R_{e,a}}{R_i}\frac{T_{te,a}}{T_{ti}}}, \quad (12)$$

Substituting eq. (11) into eq. (10), we can obtain

$$\begin{aligned}&\sigma_a\left(1+\frac{\gamma_{e,a}-1}{2}M_{e,a}^{\,2}\right)^{-\left(\frac{\gamma_{e,a}}{\gamma_{e,a}-1}\right)}(1+\gamma_{e,a}M_{e,a}^{\,2})\\ &=(\varphi_z+f)M_i\frac{A_i}{A_e}\left(1+\frac{\gamma_i-1}{2}M_i^{\,2}\right)^{-\frac{(\gamma_i+1)}{2(\gamma_i-1)}}\\ &\times\frac{1}{M_{e,b}}\left(1+\frac{\gamma_{e,b}-1}{2}M_{e,b}^{\,2}\right)^{-\frac{1}{2}}(1+\gamma_{e,b}M_{e,b}^{\,2})\\ &\times\sqrt{\frac{\gamma_i}{\gamma_{e,b}}\frac{R_{e,b}}{R_i}\frac{T_{te,b}}{T_{ti}}}.\end{aligned} \quad (13)$$

Based on eq. (8), at a given freestream Mach number, the functional dependence of Ω_z can be derived as:

$$\Omega_z = funct(\sigma_a, f, \eta, A_e/A_i). \quad (14)$$

Note that, in the above equations, the exit Mach number $M_{e,a}$, $M_{e,b}$ and the total temperature $T_{e,a}$, $T_{e,b}$ are also functions of the independent variables, as illustrated in eqs. (12), (13) and (5). By combining eqs. (11)–(13) and eq. (5), the derivative of Ω_z with respect to each independent variable can be obtained, respectively

$$\left.\frac{\partial\Omega_z}{\partial\sigma_a}\right|_{M_i,f,\eta,A_e/A_i} = \frac{\Omega_z\left(\gamma_{e,b}M_{e,b}^{\,2}-\gamma_{e,a}M_{e,a}^{\,2}\right)}{\sigma_a\left(1+\gamma_{e,a}M_{e,a}^{\,2}\right)},$$

$$\left.\frac{\partial\Omega_z}{\partial\left(A_e/A_i\right)}\right|_{M_i,f,\eta,\sigma_a} = \frac{\Omega_z\left(\gamma_{e,b}M_{e,b}^{\,2}-\gamma_{e,a}M_{e,a}^{\,2}\right)}{A_e/A_i\cdot\left(1+\gamma_{e,a}M_{e,a}^{\,2}\right)},$$

$$\left.\frac{\partial\Omega_z}{\partial\eta}\right|_{M_i,f,\sigma_a,A_e/A_i} = \frac{\Omega_z f h_{PR}}{2}\left\{\frac{\gamma_{e,a}M_{e,a}^{\,2}-\gamma_{e,b}M_{e,b}^{\,2}}{\left(C_{Pi}T_{ti}+f\eta h_{PR}\right)\left(1+\gamma_{e,a}M_{e,a}^{\,2}\right)} -\frac{\gamma_{e,b}M_{e,b}^{\,2}}{\left(1-\varphi_z\right)C_{pi}T_{ti}+f\eta h_{PR}}+\frac{\gamma_{e,b}M_{e,b}^{\,2}}{C_{Pi}T_{ti}+f\eta h_{PR}}\right\},$$

$$\begin{aligned}&\left.\frac{\partial\Omega_z}{\partial f}\right|_{M_i,\eta,\sigma_a,A_e/A_i}\\ &=\frac{-\gamma_{e,b}M_{e,b}^{\,2}\Omega_z\varphi_z}{(1+f)(1-\varphi+f)}+\frac{\Omega_z}{1+f}\frac{\gamma_{e,a}M_{e,a}^{\,2}-\gamma_{e,b}M_{e,b}^{\,2}}{\left(1+\gamma_{e,a}M_{e,a}^{\,2}\right)}\\ &-\frac{\gamma_{e,b}M_{e,b}^{\,2}\Omega_z}{2}\frac{\left(1-\varphi_z\right)\left(\eta h_{PR}-C_{pi}T_{ti}\right)}{\left(1-\varphi_z+f\right)^2C_{pe,b}T_{te,b}}\\ &+\frac{\gamma_{e,a}M_{e,a}^{\,2}\Omega_z\left(1+\gamma_{e,b}M_{e,b}^{\,2}\right)}{2\left(1+\gamma_{e,a}M_{e,a}^{\,2}\right)}\frac{\left(\eta h_{PR}-C_{pi}T_{ti}\right)}{\left(1+f\right)^2C_{pe,a}T_{te,a}}.\end{aligned}$$

Hereinafter, we will try to analyze the effects of various factors on total pressure ratio Ω_z through the above derivatives.

Replacing σ_a in eq. (13) by eq. (12), the following expression is obtained to describe the line $\Delta F/F_a=0$:

$$\begin{aligned}&\frac{(1+\gamma_{e,a}M_{e,a}^{\,2})\left[\gamma_{e,a}M_{e,a}^{\,2}\left(\frac{\gamma_{e,a}}{\gamma_{e,a}-1}+\frac{\gamma_{e,a}}{2}M_{e,a}^{\,2}\right)\right]^{-\frac{1}{2}}}{(1+\gamma_{e,b}M_{e,b}^{\,2})\left[\gamma_{e,b}M_{e,b}^{\,2}\left(\frac{\gamma_{e,b}}{\gamma_{e,b}-1}+\frac{\gamma_{e,b}}{2}M_{e,b}^{\,2}\right)\right]^{-\frac{1}{2}}}\\ &=\frac{1-\varphi_z+f}{1+f}\sqrt{\frac{C_{pe,b}T_{te,b}}{C_{pe,a}T_{te,a}}}.\end{aligned} \quad (15)$$

Based on energy equations, the difference between the exit total energy with bleed and that without bleed can be calculated as:

$$(1-\varphi_z+f)C_{pe,b}T_{te,b}-(1+f)C_{pe,a}T_{te,a} = -\varphi_z C_{pi}T_{ti} < 0. \quad (16)$$

It is thus evident that the term on the left side of eq. (15) is less than 1.0.

Defining a function as:

$$g(\gamma,\chi) = (1+\chi)\left[\chi\left(\frac{\gamma}{\gamma-1}+\frac{\chi}{2}\right)\right]^{-\frac{1}{2}}, \quad \text{where} \quad \chi=\gamma M^2.$$

Eq. (21) can be then obtained

$$\begin{aligned}g_{e,b}-g_{e,a} &\doteq \frac{\partial g}{\partial\gamma}\left(\gamma_{e,b}-\gamma_{e,a}\right)\\ &+\frac{\partial g}{\partial\chi}\left(\gamma_{e,b}M_{e,b}^2-\gamma_{e,a}M_{e,a}^2\right)>0.\end{aligned} \quad (17)$$

It is verified mathematically that the partial derivatives of function $g(\gamma, \chi)$ with respect to χ and γ are positive for the exit supersonic flow. Moreover, the specific heat ratio $\gamma_{e,b}$ with the bleed becomes lower than $\gamma_{e,a}$ without the bleed because H_2O concentration and the gas temperature will increase as the air mass flow rate entering the burner is reduced. Thus it can be inferred from eq. (17) that $\gamma_{e,b}M_{e,b}^2 > \gamma_{e,a}M_{e,a}^2$.

Apparently, $\frac{\partial \Omega_z}{\partial \sigma_a}$ and $\frac{\partial \Omega_z}{\partial (A_e/A_i)}$ are all positive, whereas both $\frac{\partial \Omega_z}{\partial \eta}$ and $\frac{\partial \Omega_z}{\partial f}$ are negative. This shows the influence of total pressure recovery σ_a, combustion efficiency η, fuel mass addition f, area ratio A_e/A_i on the engine thrust increment resulting from the bleed, as illustrated in sect. 3.

5 Mechanism of the effects of key factors on the thrust increment resulting from the bleed

The preceding sections described the effect of various factors on the thrust increment resulting from the bleed, which has also been proven mathematically. We now consider why there exist these variation rules and what the underlying mechanism is needed.

Let us analyze the relationship between the concerned factors and the engine thrust without the bleed.

The combination of eqs. (2) and (3) can establish the relationship between the engine thrust and the total pressure recovery. The first-order derivative of the dimensionless thrust F_a with respect to the total pressure recovery σ_a can then be derived as follows:

$$\frac{\partial F_a}{\partial \sigma_a} = \frac{\partial F_a}{\partial M_e}\frac{\partial M_e}{\partial \sigma_a} = \frac{A_e}{A_i}\left(1+\frac{\gamma_e-1}{2}M_e^{\,2}\right)^{-\left(\frac{\gamma_e}{\gamma_e-1}\right)} > 0. \quad (18)$$

Note that, the first-order derivative of F_a with respect to σ_a is always positive. Hence, F_a is a strictly increasing function of σ_a. The higher the total pressure recovery, the larger the engine thrust.

Furthermore, the second-order derivative of F_a with respect to σ_a is calculated as:

$$\frac{\partial^2 F_a}{\partial \sigma_a^{\,2}} = -\frac{\gamma_e M_e^{\,2}}{\sigma_a (M_e^{\,2}-1)}\frac{A_e}{A_i}\left(1+\frac{\gamma_e-1}{2}M_e^{\,2}\right)^{-\left(\frac{\gamma_e}{\gamma_e-1}\right)}. \quad (19)$$

Because the scramjet exit flow is definitely supersonic, that is, M_e is greater than 1.0, eq. (19) indicates that the second-order derivative of F_a with respect to σ_a is always negative. Dimensionless thrust F_a is a strictly increasing and concave function of the total pressure recovery σ_a. The engine thrust increases more rapidly with total pressure recovery at a lower total pressure recovery than it does at a higher total pressure recovery. Figure 11 also illustrates this trend. Engine thrust growth from σ_a=0.1 to 0.15 is much larger than that from σ_a= 0.15 to 0.2. Hence, a rise in total pressure recovery can significantly boost the engine thrust when a practical scramjet operates at a low total pressure recovery σ_a. Correspondingly, the total pressure rise because of the bleed can contribute more thrust increment at lower total pressure recovery. With the same bleed mass loss, the scramjet running at higher total pressure must reap more benefit in total pressure recovery to balance the thrust drop because of the bleed mass loss, as shown in Figure 3.

As with the above derivations, the following equations can be obtained

$$\frac{\partial^2 F_a}{\partial \sigma_a \partial \eta} = \frac{\gamma_e M_e^{\,2}\left(1+\frac{\gamma_e-1}{2}M_e^{\,2}\right)^{-\left(\frac{\gamma_e}{\gamma_e-1}\right)}}{2T_{te}(M_e^{\,2}-1)} \times \frac{A_e}{A_i}\frac{f h_{PR}}{(1+f)C_{pe}} > 0, \quad (20)$$

$$\frac{\partial^2 F_a}{\partial \sigma_a \partial f} = \frac{A_e}{A_i}\frac{\gamma_e M_e^{\,2}\left(1+\frac{\gamma_e-1}{2}M_e^{\,2}\right)^{-\left(\frac{\gamma_e}{\gamma_e-1}\right)}}{2(1+f)(M_e^{\,2}-1)} \times \frac{(1+2f)\eta h_{PR}+C_{pi}T_{ti}}{(f\eta h_{PR}+C_{pi}T_{ti})} > 0, \quad (21)$$

$$\frac{\partial^2 F_a}{\partial \sigma_a \partial (A_e/A_i)} = \frac{(1-\gamma_e M_e^{\,2})\left(1+\frac{\gamma_e-1}{2}M_e^{\,2}\right)^{-\left(\frac{\gamma_e}{\gamma_e-1}\right)}}{M_e^{\,2}-1} < 0. \quad (22)$$

Apparently, eqs. (20) and (21) exhibit similar variations of the thrust versus combustion efficiency or fuel mass addition, specifically, the heat release. The equations indicate that the total pressure recovery has more contribution to the engine thrust at higher heat release, as shown in Figure 11. Therefore, the total pressure rise due to the bleed will produce more thrust increment for the scramjet operating at higher heat release. Thus, with the same bleed mass loss, less total pressure recovery rise is sufficient for the scramjet to overcome the thrust loss resulting from the bleed when the engine operates at more heat release, as shown in Figures 5 and 7.

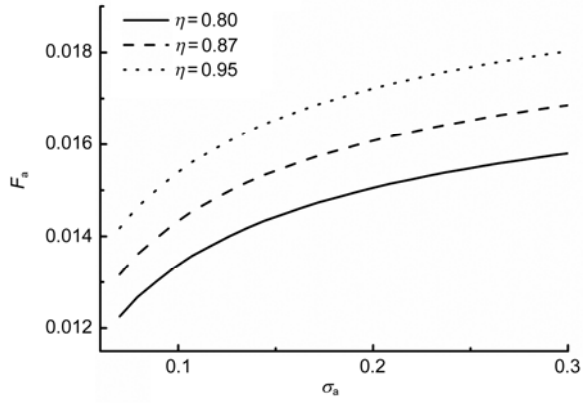

Figure 11 Dimensionless thrust vs total pressure recovery at different η.

Eq. (22) implies that the engine thrust increases more slowly with the total pressure recovery for larger area ratio, as illustrated in Figure 12. The larger the area ratio, the less thrust increment the total pressure rise contributes. With the same bleed mass loss, the scramjet needs more rise in total pressure recovery to balance the thrust drop because of the bleed mass loss for larger exit area.

The preceding analysis reveals the theoretical contribution of the boundary layer bleed to the engine thrust and the influence of total pressure recovery, combustion efficiency, fuel mass addition and area ratio of engine exit/entrance on the contribution of bleed. It helps understand the relationship among key influencing factors, the bleed and the engine thrust.

Generally, for the ground scramjet tests at Mach 6 flight condition, the total pressure recovery is about 0.07–0.1 because of flow losses and combustion heat release. The combustion efficiency in the burner is about 0.85–0.95. Thus, the engine needs a total pressure ratio of about 1.05–1.1, depending on the scramjet operating condition, to hold the thrust for a bleed mass loss of 1%. Based on our past experience in the design of boundary layer bleed system, for 1% bleed mass loss, the total pressure ratio is only 1.03–1.05 at flight speed of Mach 6.0. According to the current research in the bleed design, only the most sophisticate bleed design at an exact location might achieve a satisfactory result in which the scramjet thrust does not fall. Most bleed system would tend to reduce the scramjet thrust, though the bleed can dramatically improve the pressure recovery at high flight Mach number by relieving the loss of kinetic energy in the boundary layer. Of course, we should also concern about the aforementioned influencing factors in bleed design. A benefit or low loss in the engine thrust can be obtained by implementing the bleed at low total pressure recovery, high combustion heat release and not too large a nozzle exit. In future, it is also possible to improve scramjet performances by designing the bleed system more sophisticatedly or recycling part of the bleed flow momentum.

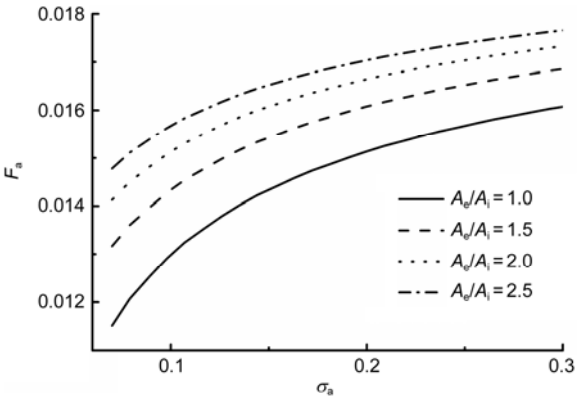

Figure 12 Dimensionless thrust vs total pressure recovery at different A_e/A_i.

6 Conclusions

The effects of boundary layer bleed on the scramjet thrust are studied in the present paper. A theoretical model is developed to evaluate the thrust increment resulting from the bleed. The influences of various factors on the thrust increment are investigated and the mechanism is subsequently discussed.

For a scramjet flying at a given freestream Mach number, the thrust increment because of the bleed is chiefly determined by the rise in total pressure recovery and the bleed mass flow rate. Some scramjet operating parameters, including initial total pressure recovery, fuel mass addition, combustion efficiency and area ratio of engine exit/entrance can affect the contributions coming from the rise in total pressure recovery and the bleed mass flow rate.

It is found that the bleed mass flow rate exerts a stronger impact on the engine thrust than the total pressure. According to current bleed design, the demand on total pressure rise offers serious challenges for the bleed design to maintain the original thrust. It seems necessary for researchers to advance some new concepts, such as designing the bleed system more sophisticatedly or recycling part of the bleed flow momentum.

Furthermore, influences of various factors are discussed. The scramjet needs a higher total pressure rise to balance the thrust drop because of the bleed mass loss at higher initial total pressure recovery or larger area ratio of engine exit/entrance. More heat release (higher combustion efficiency or larger fuel mass addition) results in a little lower demand on the rise in total pressure recovery to maintain the scramjet thrust. All these can be attributed to the variation of the engine thrust versus the above factors.

The present results help understand fundamental mechnism underlying the impact of bleeding on engine thrust.

This work was supported by the National Natural Science Foundation of China (Grant Nos. 90716014 and 91216115).

1 Riggins D W, McClinton C R, Vitt P H. Thrust losses in hypersonic engines. J Propul Power, 1997, 13(2): 281–287
2 Seddon J, Goldsmith E L. Intake Aerodynamics. New York: AIAA Education Series, AIAA, 1985. 189–216
3 Dirk Herrmann, Sergej Blem, Ali Gülhan. Experimental study of boundary-layer bleed impact on ramjet inlet performance. J Propul Power, 2011, 27(6): 1186–1195
4 Kyung Jin Ryu, Seol Lim, Dong Joo Song. A computational study of the effect of angles of attack on a double-cone type supersonic inlet with a bleeding system. Comput Fluids, 2011, 50: 72–80
5 Slater W J, Saunders J D. Modeling of fixed-exit porous bleed systems for supersonic inlets. J Propul Power, 2010, 26(2): 193–202
6 Sanders B W, Cubbison R W. "Effect of bleed-system back pressure and porous area on the performance of an axisymmetric mixed compression inlet at Mach 2.50. NASA TM X-1710. 1968
7 Syberg J, Konesek J L. Bleed system design technology for supersonic inlets. J Aircraft, 1973, 10(7): 407–413

8 Fukuda M K, Roshotko E, Hingst W R. Control of shock-wave boundary-layer interactions by bleed in supersonic mixed compression inlets. AIAA Paper, 1975, AIAA-75-1182

9 Wong W F. The application of boundary layer suction to suppress strong shock-induced separation in supersonic inlets. AIAA Paper, 1974, AIAA-74-1063

10 Wasserbauer J F, Shaw R J, Neumann H E. Minimizing boundary-layer bleed for a mixed compression inlet. AIAA Paper, 1973, AIAA-73-1270

11 Harloff G J, Smith G E. Supersonic inlet boundary layer bleed flow. AIAA J, 1996, 34(4): 778–785

12 Hamed A, Morell A, Bellamkonda G. Three-dimensional simulations of bleed-hole rows/ shock-wave/turbulent boundary-layer interactions. AIAA Paper, AIAA-2012-840

13 Hamed A, Yeuan J J, Junt Y D. Flow characteristics in boundary-layer bleed slots with plenum. J Propul Power, 1996, 12(2): 231–236

14 Chyu W J, Rimlinger M J, Shih T I-R. Control of shock-wave/ boundary-layer interactions by bleed. AIAA J, 1995, 33(7): 1239–1247

15 Tohru Mitani, Noboru Sakuranaka, Sadatake Tomioka, et al. Boundary-layer control in Mach 4 and Mach 6 scramjet engines. J Propul Power, 2005, 21(4): 636–641

16 Toshinori Kouchi, Tohru Mitani, Goro Masuya. Numerical simulations in scramjet combustion with boundary-layer bleeding. J Propul Power, 2005, 21(4): 642–649

17 Kodera M, Tomioka S, Kanda K, et al. Mach 6 test of a scramjet engine with boundary-layer bleed and two-staged fuel injection. AIAA Paper, 2003, AIAA-2003-7049

18 Häberle J, Gülhan A. Internal flowfield investigation of a hypersonic inlet at Mach 6 with bleed. J Propul Power, 2007, 23(5): 1007–1017

19 Häberle J, Gülhan A. Experimental investigation of a two-dimensional and a three-dimensional scramjet inlet at Mach 7. J Propul Power, 2008, 24(5): 1023–1034

20 Häberle J, Gülhan A. Investigation of the flow field of a 2D scramjet inlet at Mach 7 with optional boundary layer bleed. AIAA Paper, 2007, AIAA-2007-5068

21 Falempin F, Goldfeld M A, Semenova Yu V, et al. Experimental study of different control methods for hypersonic air inlets. Thermophys Aeromech+, 2008, 15(1): 1–9

22 Pandian S, Jose J, Patil M M, et al. Hypersonic air-intake performance improvement through different bleed systems. ISABE 2001-1039. 2001

23 Dirk Schulte, Andreas Henckels, Ulrich Wepler. Reduction of shock induced boundary layer separation in hypersonic inlets using bleed. Aerosp Sci Technol, 1998, 2(4): 231–239

24 Schulte D, Henckels A, Neubacher R. Manipulation of shock/ boundary-layer interactions in hypersonic inlets. J Propul Power, 2001, 17(3): 585–590

25 Weiss A, Olivier H. Behaviour of a shock train under the influence of boundary-layer suction by a normal slot. Exp Fluids, 2012, 52: 273–287

26 Chung-Jen Tam, Dean Eklund, Robert Behdadnia, et al. Investigation of boundary layer bleed for improving scramjet isolator performance. AIAA Paper, 2005, AIAA-005-3286

27 Curran E T, Murthy S N B. Scramjet Propulsion. Progress in Astronautics and Aeronautics, Vol. 189. AIAA, 2001. 483–489

28 Yu G, Li J G, Zhang X Y, et al. Experimental investigation on flameholding mechanism and combustion performance in hydrogen-fueled supersonic combustors. Combust Sci Technol, 2002, 174(3): 1–27